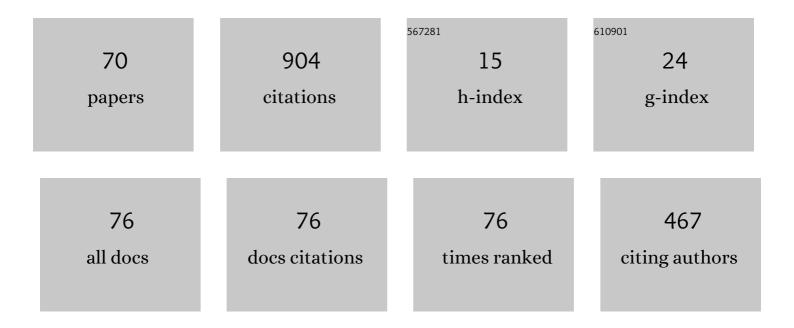
List of Publications by Year in descending order

Source: https://exaly.com/author-pdf/7748705/publications.pdf Version: 2024-02-01



MUUNLONG

#	Article	IF	CITATIONS
1	Compensation Control Model of Superheat and Cooling Water Temperature for Secondary Cooling of Continuous Casting. Steel Research International, 2011, 82, 213-221.	1.8	50
2	Numerical Analysis of Coupled Turbulent Flow and Macroscopic Solidification in a Round Bloom Continuous Casting Mold with Electromagnetic Stirring. Steel Research International, 2015, 86, 1104-1115.	1.8	48
3	Kinetic Modeling on Nozzle Clogging During Steel Billet Continuous Casting. ISIJ International, 2010, 50, 712-720.	1.4	45
4	Hydraulics and Mathematics Simulation on the Weir and Gas Curtain in Tundish of Ultrathick Slab Continuous Casting. Metallurgical and Materials Transactions B: Process Metallurgy and Materials Processing Science, 2014, 45, 392-398.	2.1	45
5	Numerical study on the characteristics of solute distribution and the formation of centerline segregation in continuous casting (CC) slab. International Journal of Heat and Mass Transfer, 2018, 126, 843-853.	4.8	40
6	Study on Mitigating Center Macro‣egregation During Steel Continuous Casting Process. Steel Research International, 2011, 82, 847-856.	1.8	38
7	Effects of Partition Coefficients, Diffusion Coefficients, and Solidification Paths on Microsegregation in Fe-Based Multinary Alloy. Metallurgical and Materials Transactions B: Process Metallurgy and Materials Processing Science, 2017, 48, 2504-2515.	2.1	28
8	Investigation of the Peritectic Phase Transition in a Commercial Peritectic Steel Under Different Cooling Rates Using In Situ Observation. Metallurgical and Materials Transactions B: Process Metallurgy and Materials Processing Science, 2020, 51, 338-352.	2.1	27
9	Longitudinal spin fluctuation contribution to thermal lattice expansion of paramagnetic Fe. Physical Review B, 2017, 95, .	3.2	25
10	Effects of Inclusion Precipitation, Partition Coefficient, and Phase Transition on Microsegregation for High-Sulfur Steel Solidification. Metallurgical and Materials Transactions B: Process Metallurgy and Materials Processing Science, 2018, 49, 3280-3292.	2.1	23
11	Mathematical Modeling of Heat Transfer in Mold Copper Coupled with Cooling Water During the Slab Continuous Casting Process. Metallurgical and Materials Transactions B: Process Metallurgy and Materials Processing Science, 2014, 45, 2442-2452.	2.1	22
12	Quantitative effects of phase transition on solute partition coefficient, inclusion precipitation, and microsegregation for high-sulfur steel solidification. Journal of Materials Science and Technology, 2019, 35, 2383-2395.	10.7	21
13	Mechanistic study of Cu-Ni bimetallic catalysts supported by graphene derivatives for hydrogenation of CO2 to methanol. Journal of CO2 Utilization, 2021, 49, 101542.	6.8	21
14	Investigation on Water Model for Fluid Flow in Slab Continuous Casting Mold With Consideration of Solidified Process. Steel Research International, 2013, 84, 31-39.	1.8	19
15	Investigations of the peritectic reaction and transformation in a hypo-peritectic steel: Using high-temperature confocal scanning laser microscopy and differential scanning calorimetry. Materials Characterization, 2019, 156, 109870.	4.4	17
16	Production of Synthetic Rutile from Molten Titanium Slag with the Addition of B2O3. Jom, 2017, 69, 1914-1919.	1.9	16
17	Effect of hot water vapor on strand surface temperature measurement in steel continuous casting. International Journal of Thermal Sciences, 2019, 138, 467-479.	4.9	16
18	Effect of uneven solidification on the quality of continuous casting slab. International Journal of Materials and Product Technology, 2013, 47, 216.	0.2	15

#	Article	IF	CITATIONS
19	Elastic properties of paramagnetic austenitic steel at finite temperature: Longitudinal spin fluctuations in multicomponent alloys. Physical Review B, 2017, 96, .	3.2	15
20	Phase Transition of Peritectic Steel Q345 and Its Effect on the Equilibrium Partition Coefficients of Solutes. Metals, 2017, 7, 288.	2.3	15
21	Numerical Analysis of Molten Pool Behavior and Spatter Formation with Evaporation During Selective Laser Melting of 316L Stainless Steel. Metallurgical and Materials Transactions B: Process Metallurgy and Materials Processing Science, 2019, 50, 2273-2283.	2.1	15
22	Study on the precipitation and coarsening of TiN inclusions in Ti-microalloyed steel by a modified coupling model. Journal of Materials Research and Technology, 2020, 9, 5499-5514.	5.8	15
23	Transient flow and mold flux behavior during ultra-high speed continuous casting of billet. Journal of Materials Research and Technology, 2020, 9, 3984-3993.	5.8	15
24	Study on the prediction of tensile strength and phase transition for ultra-high strength hot stamping steel. Journal of Materials Research and Technology, 2020, 9, 14244-14253.	5.8	14
25	A Three-Dimensional Cellular Automata Model for Dendrite Growth with Various Crystallographic Orientations During Solidification. Metallurgical and Materials Transactions B: Process Metallurgy and Materials Processing Science, 2014, 45, 719-725.	2.1	13
26	Dilatometric determination of four critical temperatures and phase transition fraction for austenite decomposition in hypo-eutectoid steels using peak separation method. Journal of Materials Research, 2018, 33, 967-977.	2.6	13
27	Quantifying the Effects of Combustion Gases' Radiation on Surface Temperature Measurements Using Two-Color Pyrometry. Energy & Fuels, 2019, 33, 3610-3619.	5.1	13
28	Thermodynamic study on the solute partition coefficients on L/δ and L/δ+γ phase interfaces for 1215 high-sulfur steel solidification by orthogonal design. Journal of Materials Research and Technology, 2020, 9, 89-103.	5.8	13
29	Evolution of Phase Transition and Mechanical Properties of Ultra-High Strength Hot-Stamped Steel During Quenching Process. Metals, 2020, 10, 138.	2.3	13
30	The Formation of Humps and Ripples During Selective Laser Melting of 316l Stainless Steel. Jom, 2020, 72, 1128-1137.	1.9	12
31	Fluid flow and heat transfer behavior of liquid steel in slab mold with different corner structures. Part 1: Mathematical model and verification. Numerical Heat Transfer; Part A: Applications, 2017, 72, 642-656.	2.1	10
32	Crystallization Behaviors of Anosovite and Silicate Crystals in High CaO and MgO Titanium Slag. Metals, 2018, 8, 754.	2.3	10
33	Stress and Friction Distribution around Slab Corner in Continuous Casting Mold with Different Corner Structures. Metallurgical and Materials Transactions B: Process Metallurgy and Materials Processing Science, 2018, 49, 866-876.	2.1	9
34	A new wavelength selection criterion for two-color pyrometer interfered with participating media. Infrared Physics and Technology, 2018, 93, 136-143.	2.9	9
35	Effect of MnS precipitation on solute equilibrium partition coefficients in high sulfur steel during solidification. Journal of Materials Research, 2018, 33, 3490-3500.	2.6	9
36	Melting and Flowing Behavior of Mold Flux in a Continuous Casting Billet Mold for Ultra-High Speed. Metals, 2020, 10, 1165.	2.3	9

#	Article	lF	CITATIONS
37	A Simple Model to Calculate Dendrite Growth Rate during Steel Continuous Casting Process. ISIJ International, 2010, 50, 1792-1796.	1.4	8
38	CuO–ZnO anchored on APS modified activated carbon as an enhanced catalyst for methanol synthesis—The role of ZnO. Journal of Materials Research, 2018, 33, 1625-1631.	2.6	8
39	Modeling on solute enrichment and inclusion precipitation during the solidification process of high sulfur steel slab. Journal of Materials Research, 2017, 32, 3854-3863.	2.6	7
40	Effect of the mold corner structure on the friction behavior in slab continuous casting molds. Journal of Materials Processing Technology, 2019, 270, 157-167.	6.3	7
41	An Approach for Modelling Slag Infiltration and Heat Transfer in Continuous Casting Mold for High Mn–High Al Steel. Metals, 2020, 10, 51.	2.3	7
42	Temperature Distribution in the As-Cast Steel Specimen During Gleeble Hot-Tensile Test and Its Effect on High-Temperature Mechanical Properties. Metallurgical and Materials Transactions B: Process Metallurgy and Materials Processing Science, 2021, 52, 1228-1242.	2.1	7
43	Universal Secondary Cooling Structure for Round Blooms Continuous Casting of Steels in Various Diameters. Steel Research International, 2015, 86, 154-162.	1.8	6
44	Study on the Fluid Flow in a Semi-Open-Stream-Poured Beam Blank Continuous Casting Mold with Submerged Refractory Funnels by Multiphase Modeling. Metals, 2016, 6, 104.	2.3	6
45	Analysis on the dynamic extension for transverse surface cracks in the as-cast steel slab at high temperatures. Engineering Failure Analysis, 2016, 66, 341-353.	4.0	6
46	Variations in the True Density and Sulfur Removal Forms of Petroleum Coke during an Ultrahigh-Temperature Desulfurization Process. Energy & Fuels, 2017, 31, 7693-7699.	5.1	6
47	Uniform Secondary Cooling Pattern for Minimizing Surface Reheating of the Strand During Round Bloom Continuous Casting. Jom, 2018, 70, 237-242.	1.9	6
48	Fluid Flow and Solidified Shell Remelting in F-EMS During Billet Continuous Casting. Jom, 2018, 70, 2059-2064.	1.9	6
49	Thermal Behavior During the Selective Laser Melting Process of Ti-6Al-4V Powder in the Point Exposure Scan Pattern. Metallurgical and Materials Transactions B: Process Metallurgy and Materials Processing Science, 2019, 50, 2804-2814.	2.1	6
50	Coupled effects of reflection and absorptive gas mixture on surface temperature determined by single color pyrometer. Journal of Quantitative Spectroscopy and Radiative Transfer, 2019, 228, 111-123.	2.3	6
51	Ab Initio Calculations on Elastic Properties of IF Steel Matrix Phase at High Temperature Based on Lattice Expansion Theory. Metals, 2020, 10, 283.	2.3	6
52	Experimental study on evolution of oxidation behavior on high-temperature continuous casting slab surface. Journal of Materials Research and Technology, 2021, 11, 2049-2058.	5.8	6
53	Fluid flow and heat transfer behavior of liquid steel in slab mold with different corner structures. Part 2: Fluid flow, heat transfer, and solidification characteristics. Numerical Heat Transfer; Part A: Applications, 2017, 72, 657-668.	2.1	5
54	Numerical modeling of centerline segregation by a combined 3-D and 2-D hybrid model during slab continuous casting. Journal of Materials Research, 2018, 33, 989-1002.	2.6	5

#	Article	IF	CITATIONS
55	Research on the Onâ€Line Simulation of a Threeâ€Dimensional Temperature Field Model of Slab Continuous Casting. Steel Research International, 2018, 89, 1800091.	1.8	5
56	Control of Coarse Precipitates of Titanium Nitride in High-Strength Low-Alloy Steel. Metal Science and Heat Treatment, 2020, 61, 534-542.	0.6	5
57	The Reduction of Cu2+ Promoted by Zn or Ni on rGO. Jom, 2020, 72, 4458-4465.	1.9	5
58	Ab Initio Study on Continuous Evolution of Mechanical Properties in Phaseâ€Transition Region of Lowâ€Carbon Steel. Steel Research International, 2020, 91, 2000070.	1.8	5
59	Temperature errors in two-color pyrometry simultaneously considering reï¬,ection and combustion gas radiation. Optics Express, 2021, 29, 25084.	3.4	5
60	Computation of Phase Fractions in Austenite Transformation with the Dilation Curve for Various Cooling Regimens in Continuous Casting. Metallurgical and Materials Transactions B: Process Metallurgy and Materials Processing Science, 2016, 47, 1553-1564.	2.1	4
61	Effect of the strand corner structure on the corner stress during the bending and straightening processes in slab continuous casting. Journal of Manufacturing Processes, 2019, 48, 270-282.	5.9	4
62	Hydraulic Modeling on Flow Behavior in High-Speed Billet Continuous Casting Mold Considering Hydrostatic Pressure and Solidified Shell. Metals, 2020, 10, 1226.	2.3	4
63	Comprehensive Utilization of Boron-Concentrate by Hydrometallurgy. Journal of Sustainable Metallurgy, 2021, 7, 244-255.	2.3	4
64	Effect of Temperature Reversion on Hot Ductility and Flow Stress–Strain Curves of C-Mn Continuously Cast Steels. Metallurgical and Materials Transactions B: Process Metallurgy and Materials Processing Science, 2015, 46, 1885-1894.	2.1	3
65	Numerical Simulation of Heat Transfer between Roll and Slab under Dry Secondary Cooling in Ultrathick Slab Continuous Casting. Steel Research International, 2020, 91, 1900516.	1.8	2
66	Experimental simulation on the high-temperature friction property of slag in slab continuous casting mold. Journal of Materials Research and Technology, 2020, 9, 6453-6463.	5.8	2
67	Thickness Distributions of Mold Flux Film and Air Gap in Billet Ultra-High Speed Continuous Casting Mold Through Multiphysics Modeling. Frontiers in Materials, 2022, 9, .	2.4	2
68	Study on Mathematical Model of Temperature and Stress for Thin Slab in Continuous Casting. , 2009, ,		1
69	Using differential scanning calorimetry to characterize the precipitation and dissolution of V(CN) and VC particles during continuous casting and reheating process. Journal of Materials Research, 2018, 33, 2784-2795.	2.6	1
70	Recovery of Vanadium from a High Ca/V Ratio Vanadium Slag Using Sodium Roasting and Ammonia Leaching. , 2014, , 613-622.		0